Supplementary Information

Hydrothermal Nickel Selenides as Efficient Electrodes in Alkaline Media: Application to Supercapacitors and Methanol Oxidation Reaction

Jiaojiao Ren,[abc] Yong Zhang,[c] Junshan Li,[c*] Junfeng Liu,[d] Jiwei Hu,[b] Chaochao Li,[b] Yun Ke,[b] Jun Zhao,[e] Andreu Cabot[fg*], Bin Tang[a*]

a State Key Laboratory of Electronic Thin Films and Integrated Devices, University of Electronic Science and Technology of China, Chengdu, 611731, China

b ChangXing HuaQiang Electronics Co., Ltd, Huzhou, 313119, China

c Institute for Advanced Study, Chengdu University, Chengdu, 610106, China

d Institute for Energy Research, Jiangsu University, Zhenjiang, Jiangsu 212013, China

e Hebei Key Laboratory of Photoelectric Control on Surface and Interface, College of Science, Hebei University of Science and Technology, Shijiazhuang 050018, China

f Catalonia Institute for Energy Research - IREC, Sant Adrià de Besòs, Barcelona, 08930, Catalonia, Spain.

g ICREA, Pg. Lluís Companys 23, Barcelona, 08010, Catalonia, Spain

Electrochemical characterization

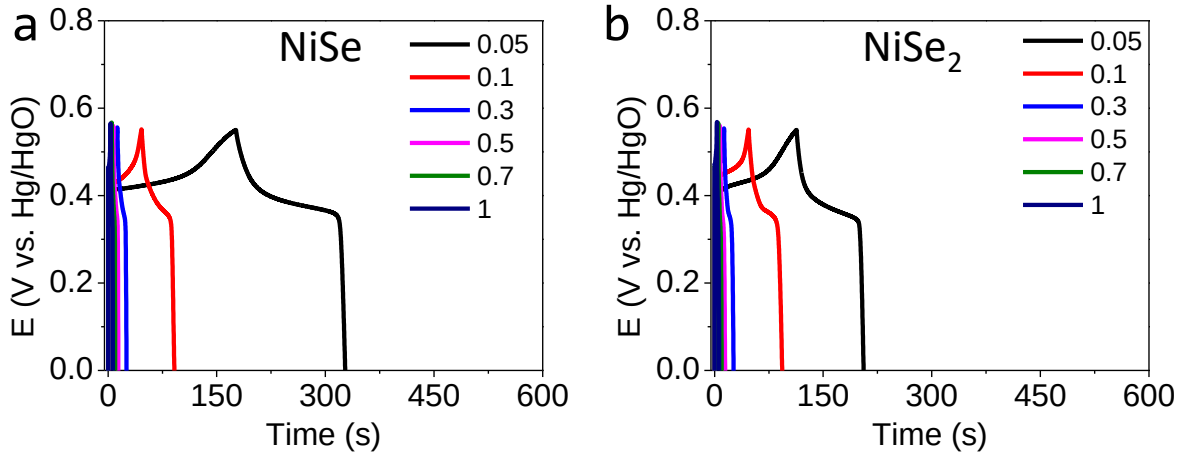

Figure S1. GCD curve for the (a) NiCSe and (b) $NiSe_2$-based electrode at a variable charge-discharge current from 0.05 mA to 1 mA.

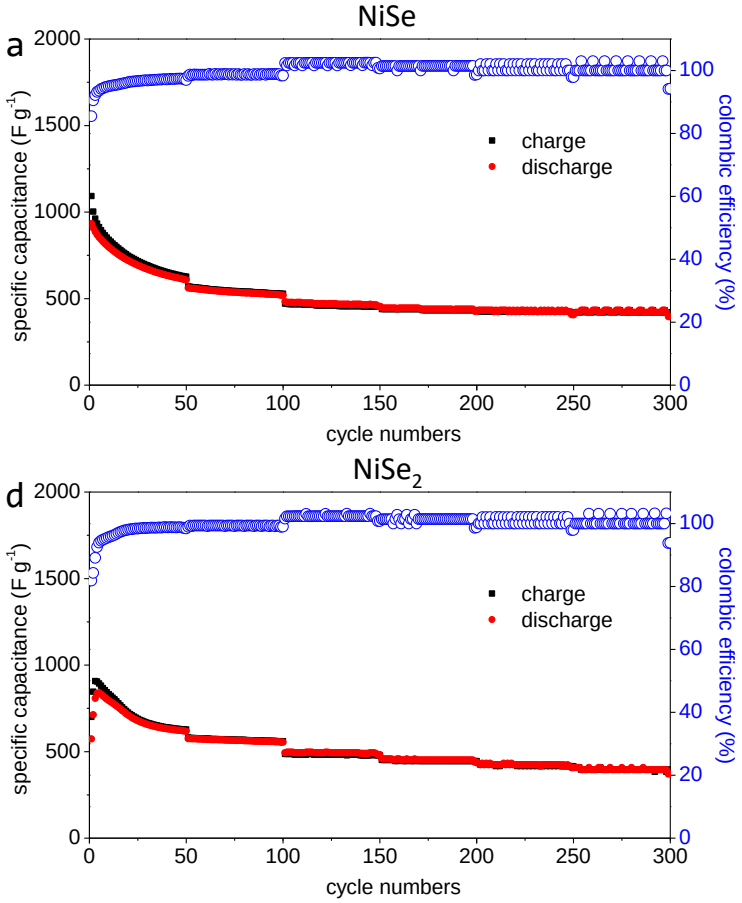

Figure S2. Specific capacitance for the (a) NiSe and (b) $NiSe_2$-based electrodes with continuous 300 cycles at a charge-discharge current of 0.05, 0.1, 0.3, 0.5, 0.7, and 1.0 mA.

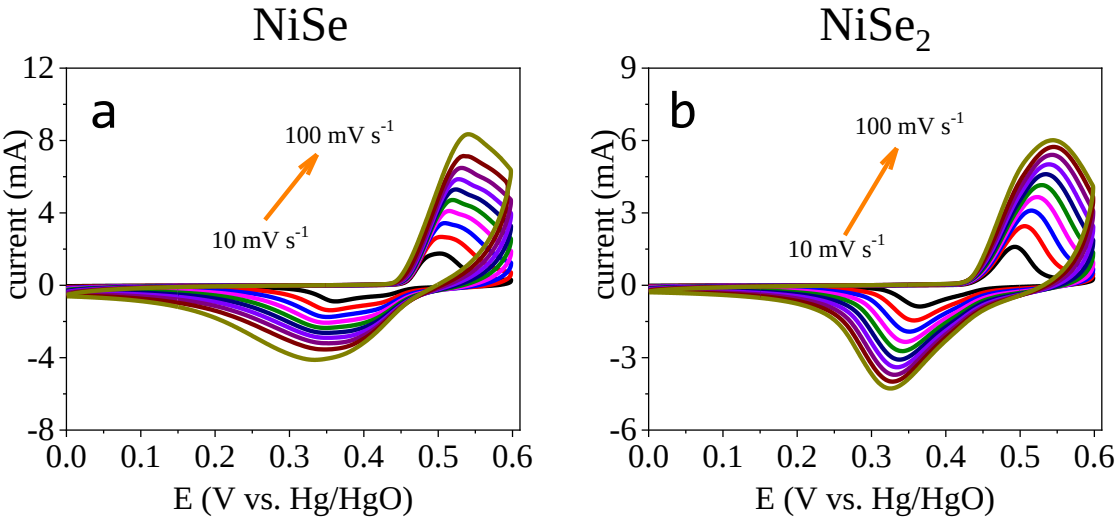

Figure S3. CV curves for (a) NiSe and (b) $NiSe_2$ based electrode at a scan rate ranging from 10 mV s^{-1} in 1 M KOH.

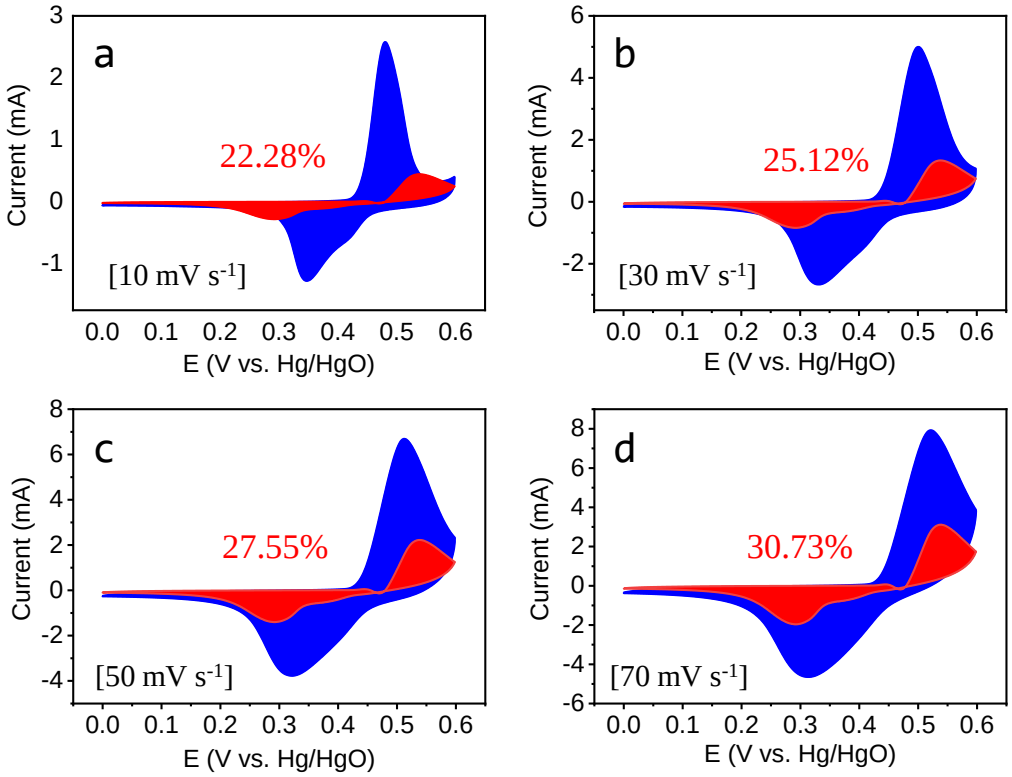

Figure S4. Capacitive contribution (red region) of Ni_3Se_4 based electrode to the total current contribution at (a) 10, (b) 30, (c) 50, (d) 70 mV s^{-1} , derived from Figure .

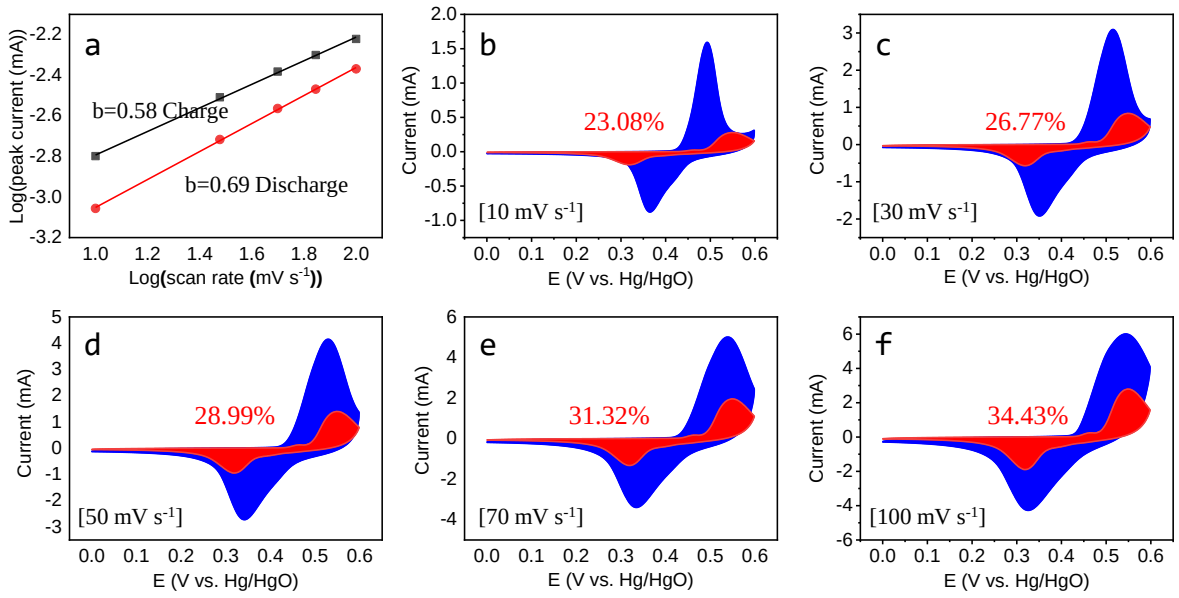

Figure S5. (a) Logarithmic dependence between peak current and scan rate at the oxidation and reduction peaks for the $NiSe_2$ based electrode. Capacitive contribution (red region) to the total current contribution at (b) 10, (c) 30, (d) 50, (e) 70, and (f) 100 mV s^{-1}.

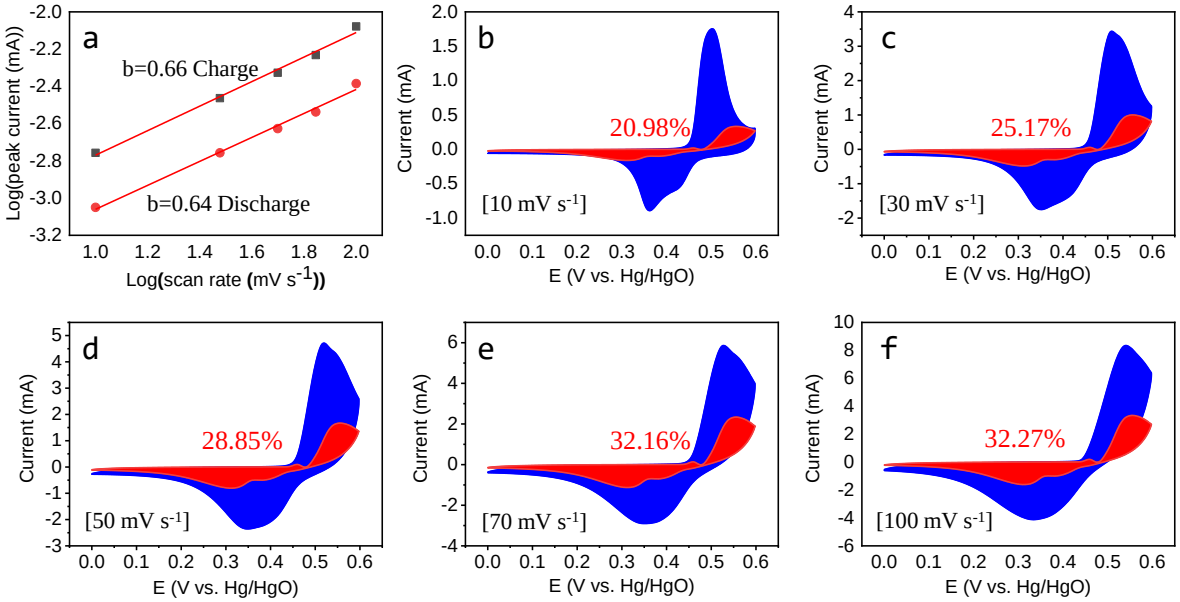

Figure S6. (a) Logarithmic dependence between peak current and scan rate at the oxidation and reduction peaks for the NiSe based electrode. Capacitive contribution (red region) to the total current contribution at (b) 10, (c) 30, (d) 50, (e) 70, and (f) 100 mV s^{-1}.

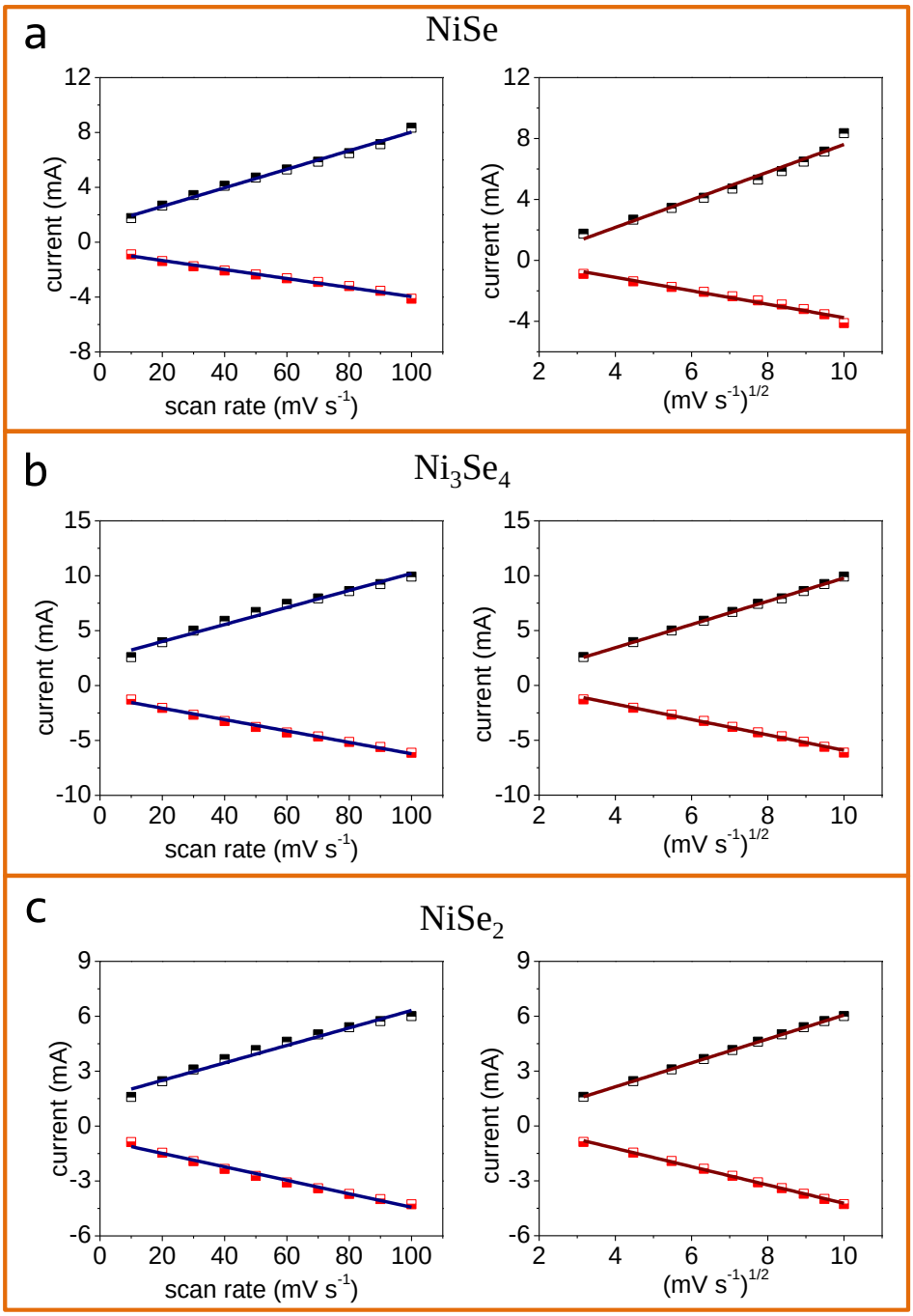

Figure S7. Determination of surface coverage of redox species (Γ*) and diffusion coefficient (D) in 1.0 M KOH for the (a) NiSe, (b) Ni_3Se_4, and (c) $NiSe_2$-based electrode.

Figures 3d and S3 show a set of CV 1.0 M KOH solution at different scan rates in 0-0.6 V versus Hg/HgO for the Ni-Se based electrodes. As it can be seen clearly in Figure S7, the current associated with both the anodic and cathodic peaks exhibits a linear increase as the scan rate is raised. Thus, the surface coverage of redox species (Γ*) was determined according to the following equation: [1]

$$I_p = \left(\frac{n^2F^2}{4RT}\right)A\Gamma^* v$$

Here, n, F, R, T, v, and A represent the number of transferred electrons (assumed to be 1), the Faraday constant (96845 C mol^{-1}), the gas constant (8.314 J K^{-1} mol^{-1}), temperature, scan rate, and the surface area of the glassy carbon electrodes (0.196 cm^2), respectively.

Furthermore, a linear relationship in Figure S7 was observed in the dependence of peak current density on the square root of the voltage scanning rate. This relationship is commonly associated with a diffusion-limited $Ni(OH)_2 \rightleftharpoons NiOOH$ redox reaction, wherein the diffusion of protons within the particle is considered to be the limiting factor governing the reaction rate. The mathematical representation of this relationship is given by: [1]

$$I_p = 2.69 \times 10^5 n^{3/2} A D^{1/2} C v^{1/2}$$

Here, I_p represents the peak current during both forward and backward scans, n denotes the number of transferred electrons (assumed to be 1), A stands for the geometric surface area of the glassy carbon (GC) electrode (0.196 cm^2), D represents the diffusion coefficient, C denotes the proton concentration (estimated to be 3.97 g cm^{-3},[2] which we approximated as 0.043 mol cm^{-3}), and v signifies the potential scan rate.

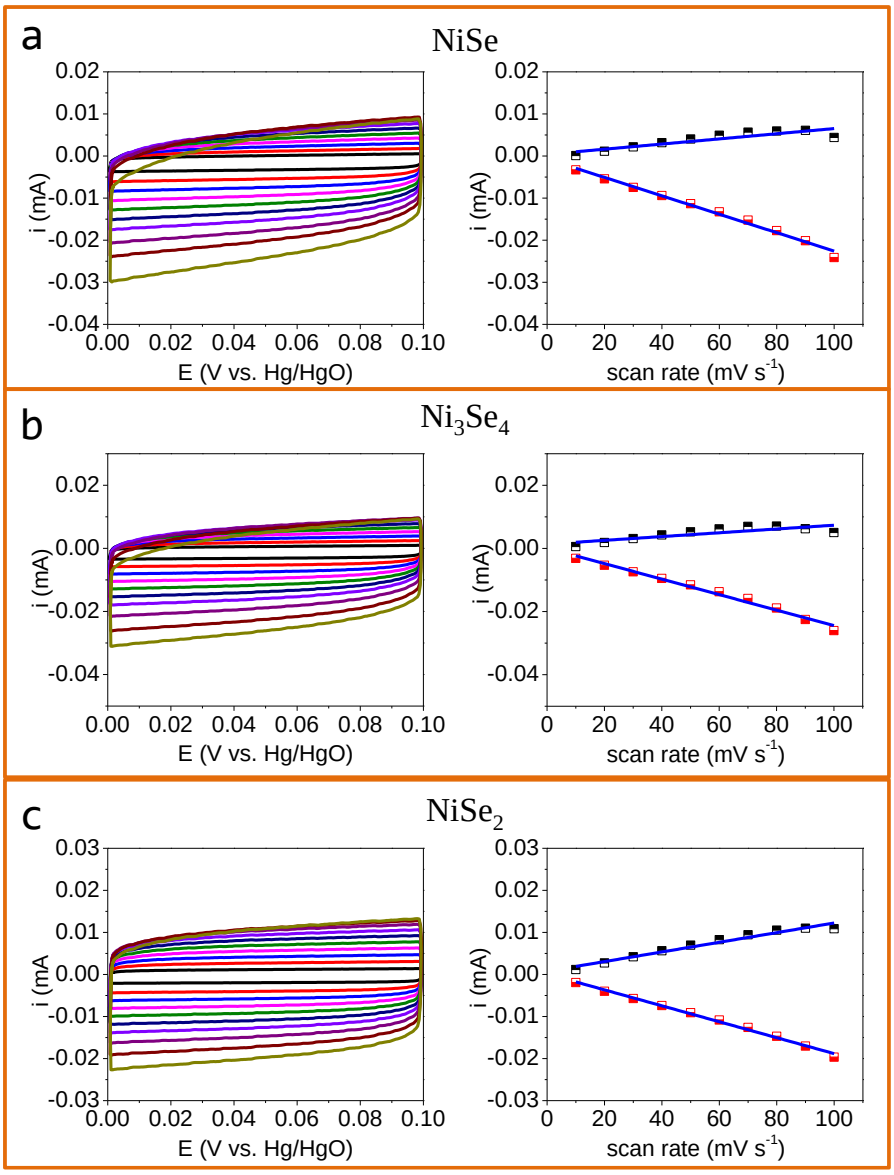

Figure S8. Determination of ECSA curves in 1 M KOH for the (a) NiSe, (b) Ni_3Se_4, and (c) $NiSe_2$-based electrode.

The Electrochemically Active Surface Areas (ECSA) were determined by assessing the electrochemical double-layer capacitance (C_{dl}), derived from CVs with various scan rates. As shown in Figure S8, by plotting the capacitive current (I) against the scan rate (v), a linear relationship emerged with the slope corresponding to C_{dl}. Thus, the ECSA can be determined utilizing the equation[3]:

$$ECSA = C_{dl}/C_s$$

where Cs is determined to be 0.04 mF cm^{-2} based on reported values for Ni-based metal electrodes in aqueous alkaline solution. [4]

Table S1. The intrinsic property and the supercapacitive and the MOR performance.

materials and morphology	crystal system	space group	[a] I^* (mol cm^{-2})	[a] D (cm^2 s^{-1})	[a] ECSA (cm^{-2})	[a] supercapacitance (F g^{-1} @0.5 mA)	[b] MOR (mA cm^{-2}@0.6 V)
NiSe nanoparticles	Monoclinic	P 63/m m c	5.35×10^{-8}	3.42×10^{-9}	8.5	451.3	56.9
Ni_3Se_4 nanorods	Hexagonal	C 1 2/m 1	6.88×10^{-8}	5.83×10^{-9}	9.2	612.0	93.7
$NiSe_2$ cubics	Cubic	P a -3	4.51×10^{-8}	2.53×10^{-9}	9.1	438.9	68.5

Note that the values of a were taken in 1 M KOH, and b was recorded in the 1 M KOH containing 1 M methanol.

Reference

[1] A.J. Bard, L.R. Faulkner, Electrochemical Methods: Fundamentals and Applications, 2nd ed., 2001.

[2] S.J. Zhang, Y.X. Zheng, L.S. Yuan, L.H. Zhao, Ni-B amorphous alloy nanoparticles modified nanoporous Cu toward ethanol oxidation in alkaline medium, J. Power Sources. 247 (2014) 428–436. https://doi.org/10.1016/j.jpowsour.2013.08.129.

[3] C.C.L. McCrory, S. Jung, I.M. Ferrer, S.M. Chatman, J.C. Peters, T.F. Jaramillo, Benchmarking Hydrogen Evolving Reaction and Oxygen Evolving Reaction Electrocatalysts for Solar Water Splitting Devices, J. Am. Chem. Soc. 137 (2015) 4347–4357. https://doi.org/10.1021/ja510442p.

[4] C.C.L. McCrory, S. Jung, J.C. Peters, T.F. Jaramillo, Benchmarking Heterogeneous Electrocatalysts for the Oxygen Evolution Reaction, J. Am. Chem. Soc. 135 (2013) 16977–16987. https://doi.org/10.1021/ja407115p.